Journal of Controlled Release 277 (2018) 48–56

Contents lists available at ScienceDirect

Journal of Controlled Release

journal homepage: www.elsevier.com/locate/jconrel

EV20-mediated delivery of cytotoxic auristatin MMAF exhibits potent therapeutic efficacy in cutaneous melanoma

Emily Capone[a], Alessia Lamolinara[b], Daniela D'Agostino[a], Cosmo Rossi[c], Vincenzo De Laurenzi[a], Manuela Iezzi[b], Stefano Iacobelli[d], Gianluca Sala[a,d,*]

[a] Department of Medical, Oral and Biotechnological Sciences, University of Chieti-Pescara, Chieti, Italy
[b] Department of Medicine and Aging Science, CeSi-Met, University of Chieti-Pescara, Chieti, Italy
[c] Aging Research Center and Translational Medicine (CeSI-Met), Italy
[d] MediaPharma s.r.l., Via della Colonnetta 50/A, Chieti, Italy

ARTICLE INFO

Keywords:
Antibody-drug conjugate (ADC)
HER-3
Melanoma
BRAF
Vemurafenib

ABSTRACT

Cutaneous melanoma is one of the cancers with the fastest rising incidence and in its advanced metastatic form is a highly lethal disease. Despite the recent approval of several new drugs, the 5-year overall survival rate for advanced cutaneous melanoma is still below 20% and therefore, the development of novel treatments remains a primary need. Antibody-Drug Conjugates are an emerging novel class of anticancer agents, whose preclinical and clinical development has recently seen a remarkable increase in different tumors, including melanoma. Here, we have coupled the anti-HER-3 internalizing antibody EV20 to the cytotoxic drug monomethyl auristatin F (MMAF) to form a novel antibody-drug conjugate (EV20/MMAF). In a panel of human melanoma cell lines, this novel ADC shows a powerful, specific and target-dependent cell killing activity, independently of BRAF status. Efficacy studies demonstrated that a single administration of EV20/MMAF leads to a long-lasting tumor growth inhibition. Remarkably, the effect of this novel ADC was superior to the BRAF inhibitor vemurafenib in preventing kidney, liver and lung melanoma metastases. Overall, these results highlight EV20/MMAF as a novel ADC with promising therapeutic efficacy, warranting extensive pre-clinical evaluation in melanoma with high levels of HER-3 expression.

1. Introduction

The incidence of Cutaneous Melanoma (CM) has been rising dramatically over the last 50 years, especially in industrialized and western countries [1]. Although early-stage CM can be managed by surgery, advanced metastatic disease is extremely hard to cure and treatment options are largely unsatisfactory, making the search for effective cure an urgent need [2]. In the recent past, a remarkable step forward in the treatment of advanced CM has been achieved thanks to the introduction of checkpoint inhibitors (CTLA-4 and PD-1 blocking antibodies) and therapeutics blocking the oncogenic BRAF/MAPK signaling axis [3,4]. Indeed, approximately 50% of CM harbors activating BRAF gene mutations (over 90% of which are V600E) which can be specifically targeted by vemurafenib. However, patients rapidly develop resistance to this drug, with different mechanisms [5]. One of the better characterized escape mechanisms is driven by the up-regulation of HER-3, a member of the EGF receptor family (HERs) [6]. This receptor has been known to play a crucial role in modulating the sensitivity of targeted therapeutics in different cancers, such EGFR inhibitors in lung cancer, HER-2 and PI3K inhibitors in breast cancer and RAF/MEK inhibitors in melanoma [7–12]. This has prompted the use of antibodies targeting HER-3, both as a single agent or in combination with anti-cancer drugs to overcome resistance. However, this approach turned out to have modest therapeutic activity [13–15].

Antibody-Drug Conjugates (ADCs) are an emerging novel class of anticancer agents, whose preclinical and clinical development have recently seen a remarkable increase in different cancers, including melanoma [16–21]. Recently, we developed the first generation HER-3 based ADC coupling the plant toxin saporin to EV20, a humanized internalizing anti-HER-3 antibody generated by our group [22–24]. This ADC showed the ability to efficiently deliver the toxin in HER-3 dependent manner. Here, we further investigated the clinical potentiality of this approach by generating a novel ADC based on EV20 coupled to the tubulin polymerization inhibitor monomethyl auristatin F (EV20/MMAF). We confirmed that EV20 is able to serve as a partner of the ADC to deliver cytotoxic drugs to HER-3 expressing cells. Interestingly,

* Corresponding author at: Department of Medical, Oral, and Biotechnological Sciences, Center of Excellence on Aging and Translational Medicine (CeSi-Met), Via dei Polacchi 11, 66100 Chieti, Italy.
E-mail address: g.sala@unich.it (G. Sala).

https://doi.org/10.1016/j.jconrel.2018.03.016
Received 27 December 2017; Received in revised form 7 March 2018; Accepted 13 March 2018
Available online 14 March 2018

EV20/MMAF displayed potent and specific in vitro cell killing activity in melanoma cells, independently of BRAF status. Finally, in vivo efficacy studies revealed this novel ADC possesses superior activity compared to BRAF inhibitor vemurafenib in curing kidney, liver and lung melanoma metastases.

2. Materials and methods

2.1. Reagents

Antibodies were as follows: phosphorylated ErbB-3 (Tyr1289) and ErbB-3 from Cell Signaling Technology (Danvers, MA); while anti-actin was purchased from Sigma-Aldrich Corporation (St Louis, MO). Neuregulin-1β (NRG-1β) was purchased from R&D Systems, Inc. (Minneapolis, MN). PLX4720 and vemurafenib (PLX4032) were purchased from Selleck Chemicals (Houston, TX 77054 USA). EV20 antibody was produced as described [23]. Murine anti-MMAF antibody and donkey anti-human IgG were purchased from Levena Biopharma (San Diego, CA, USA) and Jackson Immuno Research (Baltimore, PA, USA), respectively. Recombinant human ECD ErbB-3 was from ACROBiosystems (Bethesda, MD). (3-(4,5-Dimethylthiazole-2-yl)-2,5 diphenyltetrazolium bromide (MTT) was purchased from Sigma-Aldrich Corporation. Free MMAF was purchased from MedChemExpress (NJ 08852, USA).

2.2. Cell lines

Melanoma (A375m, SK-MEL 2, WM852, WM115, and C8161) cell lines were kindly provided and authenticated by the lab of Prof. Alex Ullrich (The Max-Planck Institute, Martinsried, Germany) in 2013. MDA MB 231 triple negative breast cancer cell line was purchased from ATCC. Her-2/neu positive TUBO cell line has been originally isolated from a carcinoma arising in a BALB-neuT mouse [25]. All cell lines were cultured < 3 months after resuscitation. All cells were grown with media according to manufacturer's (ATCC) instructions supplemented with 10% heat-inactivated fetal bovine serum (FBS; Invitrogen), L-glutamine, 100 units/ml penicillin, and 100 μg/ml streptomycin (Sigma-Aldrich Corporation, St. Louis, MO, USA), and incubated at 37 °C in humidified air with 5% CO2. For WM852 cell line medium was supplemented with 2% FBS and 5 μg/ml insulin. Expression of ectopic HER-3 in MDA MB 231 HER-3 cells was obtained by infection with stocks of LTR and LTR HER-3 recombinant retrovirus as described [26].

2.3. Generation of EV20/MMAF (Levena)

EV20/MMAF ADC described in this study was generated and characterized by LEVENA Biopharma (San Diego, CA). The EV20 humanized anti-HER-3 antibody was previous described [22,23]. The conjugation process of the linker-functionalized MMAF to EV20 was performed by LEVENA Biopharma (San Diego, CA, USA) using the “SeaGen” conjugation method (Patent US 7659241). The drug/antibody ratio (DAR) was determined by HIC (Hydrophobic interaction chromatography) based on SH/Ab ratio, and for the EV20/MMAF ADC used in this study ranged between 4 and 5. HIC-HPLC analysis was performed on ThermoFisher MabPac HIC-10 LC column. Buffer A (20 mM sodium phosphate, 1.5 M Ammonium Sulfate, pH 7.0) and Buffer B (20 mM sodium phosphate, 25% v/v isopronol, pH 7.0) were used on Agilent 1100 HPLC. Aggregation was determined by SEC-HPLC (size exclusion chromatography) and resulted below 2% in all preparations. SEC-HPLC analysis was performed on Tosoh TSKgel G3000SW-XL, 7.8mmx30cm, 5 mm. Buffer A (150 mM sodium phosphate, 300 mM sodium chloride, pH 7.0, 30 min 1.5 M Ammonium Sulfate, pH 7.0) was used on Agilent 1100 HPLC. The amount of free drug was determined by RP-HPLC (Reversed phase chromatography) while amount of unconjugated antibody by HIC-HPLC. In all preparations used in this study, levels of free toxin were negligible and the percentage of the unconjugated antibody below 2%. RP-HPLC analysis was performed on Zorbax Eclipse XDB-C18, 4.6x150mm, 5 μ Column Temp: 50 °C. Buffer A (water +0.05%TFA) Buffer B (Acetonitrile +0.045% TFA) were used on Agilent 1100 HPLC.

2.4. LC-MS (liquid chromatography mass Spectometry) analysis of released payload in mice serum

For evaluation of released payload in mice serum, CD1 nude mice were injected intravenously with 3.3 mg/kg of EV20/MMAF and blood samples collected thereafter at the following time points:

1 min, 5 min, 1 h, 24 h and 72 h. LC-MS analysis of free MMAF was performed by Toscana Life Sciences (http://www.toscanalifesciences.org/it/) as detailed below.

Plasma samples (100 μl) were treated with 200 μl of ACN:MeOH (50/50, v/v) in order to precipitate proteinaceous materials. The supernatant was recovered by centrifugation at 4000 x g for 20 min at 4 °C, evaporated to dryness under nitrogen stream. One hundred μl of 0.1% formic acid in H_2O:ACN (90:10, v/v) was added to each vial. Samples (10 μl) were analyzed by HPLC-MS/MS using a CSH C18 130 Å column (1 mm × 150 mm, 1.7 μm, Waters), at 50 °C and with a flow rate of 0.1 ml/min in gradient mode. Mobile phase A consisted of 0.1% formic acid in water and mobile phase B of 0.1% formic acid in ACN. The following gradient was used: 10% B for 1 min, 10%–100% in 7 min, holding at 100% B for 1 min and re-equilibration at 10% B for 10 min. For each sample the LC-ESI-MS/MS runs were performed in triplicate. The detector was a Q-Exactive Plus mass spectrometer (Thermo Scientific) operating in positive ion mode with the following parameters: capillary temperature, 320 °C; spray voltage, 2.7 kV; sheath gas (nitrogen), 5, resolution, 70.000; AGC target, 2e5; Maximum IT, 100 ms; Isolation window, m/z 2.0; Scan range, m/z 150–2000; NCE, 24. Parallel reaction monitoring (PRM)-based targeted mass spectrometry was used to quantitative determination of MMAF. The protonated molecular ions at m/z 732.4909 was selected and the fragmentation pathway yielding the ion at 700.4639 was monitored. The acquisition software was XCalibur, version 3.0.63 (Thermo Scientific). The detection limit of free MMAF in the assay resulted to be 0.07 nM.

2.5. Elisa

Recombinant HER-3 extracellular domain (ECD) or the mouse anti-MMAF antibody were used as capturing antigen to evaluate ADC in vitro binding. Ninety-six well-plates NUNC Maxisorp modules were coated with the antigen (1 μg/ml) overnight at 4 °C. After blocking with 1% BSA in PBS at room temperature for 1 h, increasing concentrations of EV20 or EV20/MMAF were added and incubated at room temperature for 1 h. After several washes with PBS + 0,05% Tween-20, a goat anti-human IgG-HRP solution (Sigma-Aldrich Corporation) was added to each well and incubated at room temperature for 1 h. After washes, stabilized chromogen was added to each well for at least 10 min in the dark, then the reaction was stopped with the addition of 1 N H_2SO_4 and the resulting colour read at 450 nm with an Elisa reader. The *Kd* values were calculated using GraphPad Prism 5 software.

For pharmacokinetic studies, non-tumor bearing Athymic CD-1 nu/nu mice (n = 3) were injected intravenously with a single dose of EV20/MMAF (3.3 mg/kg) and blood samples collected at different time points (1 min; 5 min; 1 h, 24 h; 72 h; 168 h and 240 h). Serum concentrations of total EV20 and intact ADC were measured by sandwich ELISAs using as capture antigen donkey anti-human IgG or mouse anti-MMAF antibody respectively, and goat anti-human IgG-HRP for detection. Half-time ($t_{1/2}$) and AUC values were obtained by Kinetica 5.0 software.

2.6. FACS analysis

For receptor surface expression analysis, flow cytometry was

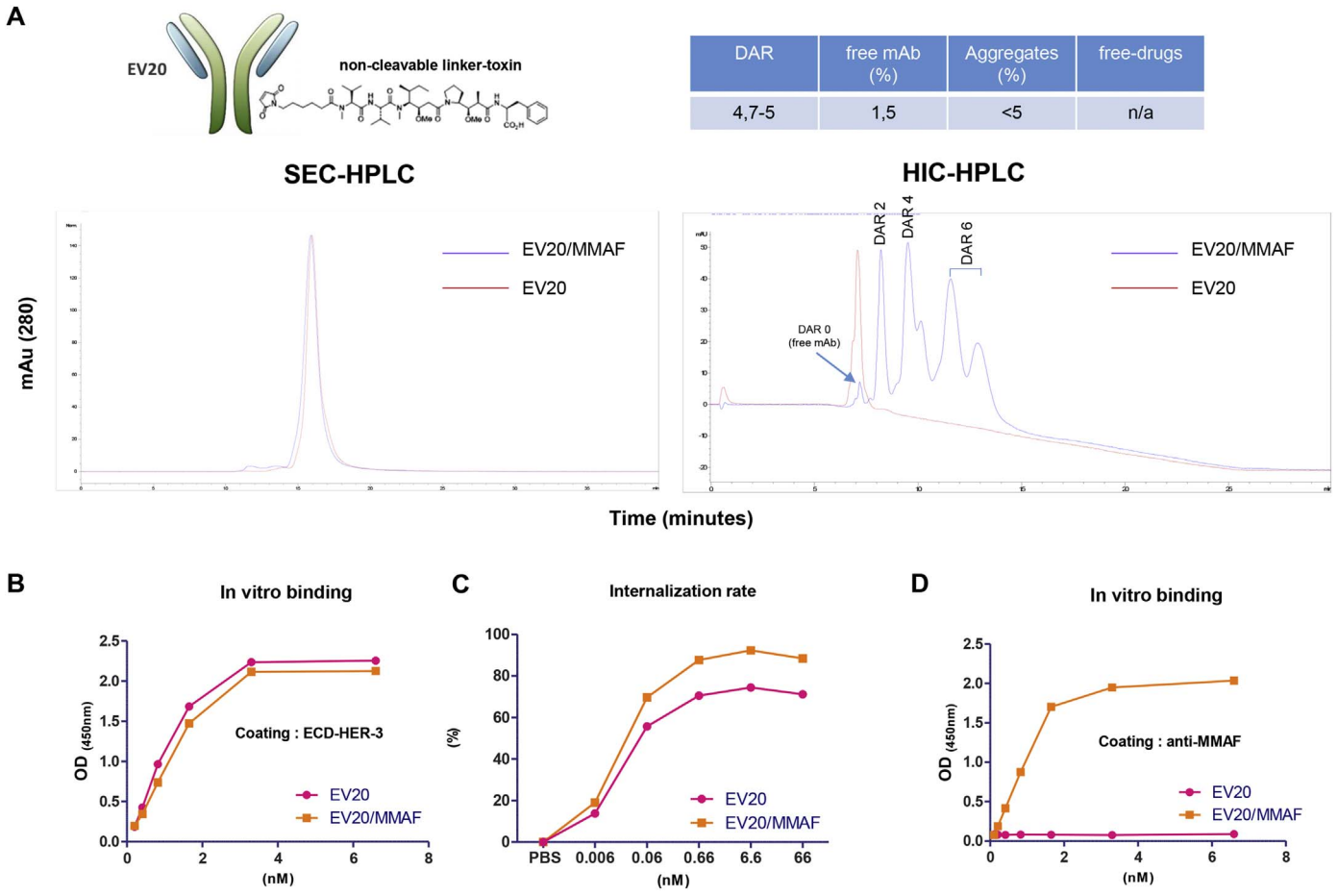

Fig. 1. Generation and characterization of EV20/MMAF.
(A) Schematic representation of EV20/MMAF ADC and Table indicating ADC information. Representative SEC and HIC-HPLC analysis of naked and conjugated antibodies are shown. (B) in vitro binding affinity of naked and MMAF-conjugated EV20 antibodies. ELISA was performed using as capture antigen the HER-3 extra cellular domain (ECD) and bound EV20 or EV20/MMAF antibodies were detected by HRP-labelled goat anti-human IgG. *Kd* values (EV20: 1.63 nM; EV20/MMAF: 1.62 nM) were calculated using Graphpad Prism 5 software. (C) Internalization assay. Human melanoma cells were exposed to increasing concentrations of EV20 and EV20/MMAF for 6 h at 37 °C and then HER-3 surface expression analyzed by FACS. EC_{50} values (EV20: 0.018 nM; EV20/MMAF: 0.018 nM) were calculated using Graphpad Prism 5 software. (D) Sandwich ELISA was performed using the murine anti-MMAF antibody as capture antigen and HRP-labelled goat anti-human IgG for detection. *Kd* value (EV20/MMAF: 1.43 nM) was calculated using Graphpad Prism 5 software.

performed according to standard procedures. About one million cells were harvested and labelled with EV20 or trastuzumab on ice for 30 min. Cells were then washed with 2 ml PBS, pulled down, and stained with anti-Human Fc PE-conjugate as secondary antibody (Molecular Probes, Life Technologies). Analysis was performed using FACSCantoII cytometer (Becton Dickinson, Buccinasco, MI, Italy).

2.7. Internalization assay

A375m cells were plated in 12 well-plates and grown in 10% FBS DMEM for 24 h. Cells were then incubated with increasing doses of EV20 or EV20/MMAF for 6 h for dose-dependent assay; then, flow cytometry assay in order to evaluate HER-3 surface expression was performed as described [23]. EC_{50} values were calculated using GraphPad Prism 5 software.

2.8. Cell cycle analysis

After the indicated treatments and times, ~ 2×10^6 cells were harvested and centrifuged for 5 min. Then, PBS was added to the cells followed by 70% ethanol to bring the final volume at 0.5 ml. The cells were stored overnight at 4 °C. Cells were centrifuged, washed twice with PBS, before resuspending and staining them with 0.5 ml propidium iodide (PI, 50 μg/ml) and RNAase (10 μg/ml) at 4 °C overnight in the dark. Cell cycle analysis was performed using FACSCantoII cytometer (Becton Dickinson, Buccinasco, MI, Italy). Data were analyzed using FCSExpress 5 software.

2.9. Annexin V staining

SK-MEL 2 melanoma cells were incubated with EV20-Sap at the dose of 0.6 nM or PBS as control. After 72 h, 1×10^5 cells were harvested, washed with PBS and stained with 0.5 μl of APC AnnexinV (BD Biosciences Pharmingen) and 5 μl of 7-Amino-Actinomycin D (7-AAD) for 30 min at RT. Finally, Binding Buffer was added and samples were analyzed using FACSCantoII cytometer (Becton Dickinson, Buccinasco, MI, Italy).

2.10. Cytotoxicity assays

Cell proliferation was assessed by MTT [3-(4,5-dimethyldiazol-2-yl)-2,5-diphenyl tetrazolium bromide] assay (Sigma-Aldrich). Cell lines were seeded into 24-well plates at a density of 5×10^3 cells/well in 500 μl of complete culture medium, cells were treated with drugs at indicated concentration in triplicates and further incubated for 120 h. At the end of the incubation period, cells were incubated with 200 μl of MTT solution (medium serum free with 0.5 mg/ml of MTT) for further 2 h. After removal of MTT solution, 200 μl of dimethyl sulfoxide (DMSO) was added to the wells for 10 min and the absorption value at 570 nm was measured using a multi-plate reader. All experiments were

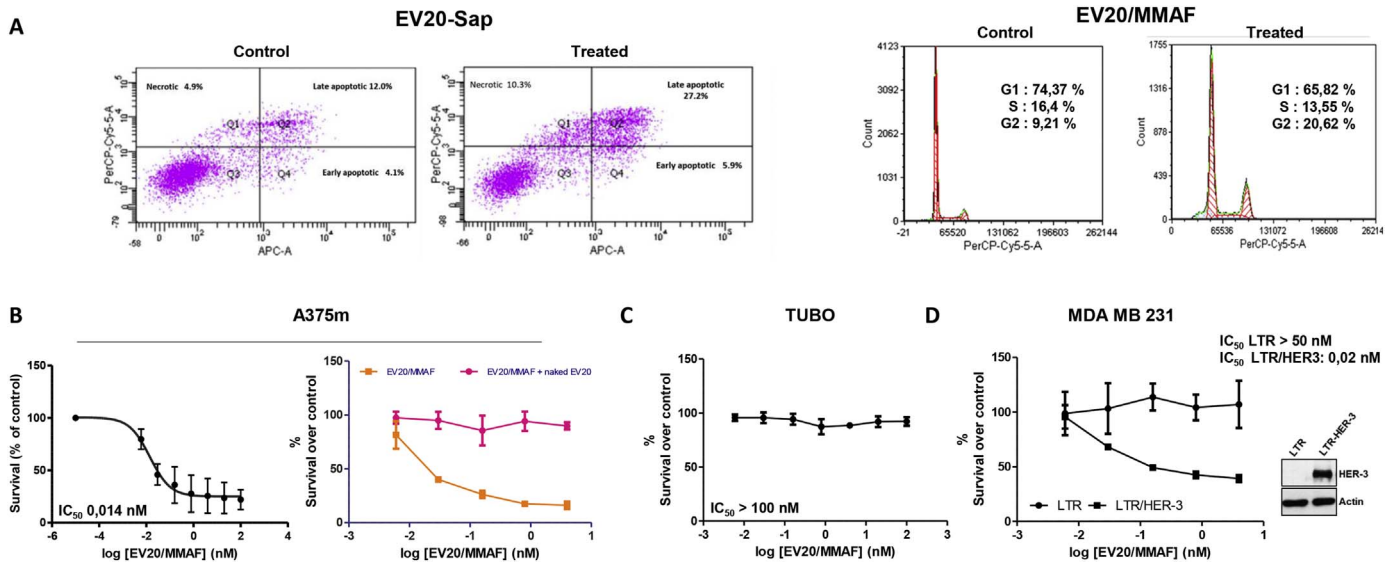

Fig. 2. EV20/MMAF displays potent and specific in vitro cell killing activity.
(A) SK-MEL 2 cells were treated with 0.6 nM of EV20-Sap for 72 h and the apoptosis rate was evaluated with AnnexinV-APC/7AAD staining (left panel). HER-3+ A375m were treated for 48 h with 1 nM of EV20/MMAF in complete medium. Flow cytometry cell cycle analysis using propidium iodide DNA staining is shown (right panel). (B) The cytotoxic response of A375m cells to EV20/MMAF treatment was evaluated by MTT after 120 h of drug exposure. IC_{50} was calculated with GraphPad Prism 5 software(left panel). A375m cells were incubated for 120 h with increasing doses of EV20/MMAF alone or with 500-fold molar excess of naked EV20 and proliferation was evaluated by MTT assay (right panel). (C) HER-3+ BALB-neu T mouse-derived cells (TUBO) were incubated for 120 h with increasing doses of EV20/MMAF and proliferation was evaluated by MTT assay. (D) MTT assay showing EV20/MMAF activity in triple negative HER-3 negative MDA MB 231 breast cancer cells after ectopic expression of HER-3 by retroviral stock infections. Western blotting confirming HER-3 overexpression in LTR-HER-3 infected cells is shown. For all MTT assays data are expressed as % survival over control. Mean +/− SD (n = 3). IC_{50} values were calculated with GraphPad Prism 5 software.

performed in quadruplicate. *p* values were determined by Student's *t*-test and considered significant for $p < 0.05$. For competition assays cells were seeded in 24-wells plate at a density of 5×10^3 cells/well in 10% fetal bovine serum-containing medium and allowed to attach and propagate overnight before the treatments. Then, increasing doses of EV20/MMAF and 500-fold excess of *naked* EV20 was added to the medium. After 5 days, the cells were incubated with MTT (final concentration of 0.5 mg/ml) at 37 °C for 2 h. Spectrophotometric absorbance of the samples was determined at 570 nm.

For drug combination assays (EV20/MMAF + PLX4720), individual dose response curves and combination curve with PLX4720 at a non costant-ratio were obtained after 120 h drugs exposure in A375m cells. We entered the combination proliferation data, along with the data obtained from single drug treatments, into Calcusyn software (Biosoft, Cambridge, UK) [27,28] to determine a combination index value (CI) for each combination point, which quantitatively defines additivity (CI = 1), synergy (CI < 1), and antagonism (CI > 1).

Free MMAF cell killing activity was evaluated by MTT assays in SK MEL-2 HER-3 positive and C8161/WM852 HER-3 negative melanoma cell lines. Dose response curves were obtained after 120 h of drug exposure. Experiments were performed in triplicate and IC_{50} values were calculated using GraphPad Prism 5 software.

2.11. Immunochemistry

Lysates from cells in culture were prepared by washing cells twice in cold PBS followed by lysis with RIPA lysis buffer supplemented with protease and phosphatase inhibitors (Sigma-Aldrich Corporation) for 10 min at 4 °C. Insoluble materials were removed by centrifugation (13,000 rpm for 10 min at 4 °C) and protein concentration was assessed by the method of Bradford. Immunoblotting was performed as described [22].

2.12. In vivo tumor growth

Athymic CD-1 nu/nu mice (5 or 7 weeks old) were purchased from Charles River Laboratories (Calco, Italy) and maintained under specific pathogen-free conditions with food and water provided ad libitum. The animal health status was monitored daily. Procedures involving animals and their care were conducted according to institutional guidelines in compliance with national and international laws and policies (Authorization n° 292/2017-PR). A375m xenograft model was generated by subcutaneous injection into the right flank of mice of 5×10^6 of cells in 200 µl of PBS. When xenografts became palpable, animals were divided into 4 groups (n = 6) in a way to provide a similar range of tumor size for each group. The treated group received intravenous injections of increasing doses of EV20/MMAF in PBS (1.1–3.3-10 mg/kg) whereas the control group received PBS only. Tumor volume was monitored every week by a caliper and calculated by the following formula: tumor volume (mm^3) = (length × width^2)/2. A tumor volume of 1.5 cm^3 was chosen as endpoint for both experiments after which mice were sacrificed. Survival curves were derived from Kaplan-Meier estimates and compared by log-rank test (GraphPad Prism 5). EV20/MMAF accumulation in tumor tissue was evaluated by immunofluorescence analysis of A375m tumor xenografts. Animals bearing A375m tumors received a single injection of PBS (as a control), or EV20/MMAF at the dose of 3.3 mg/kg and thereafter animals were sacrificed 1 h, 24 h, 48 h and 72 h later. Fresh tumor tissues were frozen in a cryo-embedding medium (OCT, BioOptica) and cryostat sections were incubated with the following antibodies: rat monoclonal anti-CD31 (550,274, BD Pharmingen) mixed with rat monoclonal anti-CD105 (550,546, BD Pharmingen), followed by secondary antibody conjugated with Alexa 546 (Molecular Probes, Life Technologies) and AlexaFluor-488 conjugated anti-human IgG (Invitrogen, Life Technologies). Nuclei were stained with DRAQ5 (Alexis, Life Technologies). Image acquisition was performed using Zeiss LSM 510 META confocal microscope.

2.13. Experimental metastasis assay in NOD scid gamma (NSG) mice

NSG mice were purchased from Jackson Laboratory and bred in the animal facility of CeSI-Met, G. D'Annunzio University, Chieti. Animal care and experimental procedures were approved by the Ethics Committee for Animal Experimentation of the institute according to

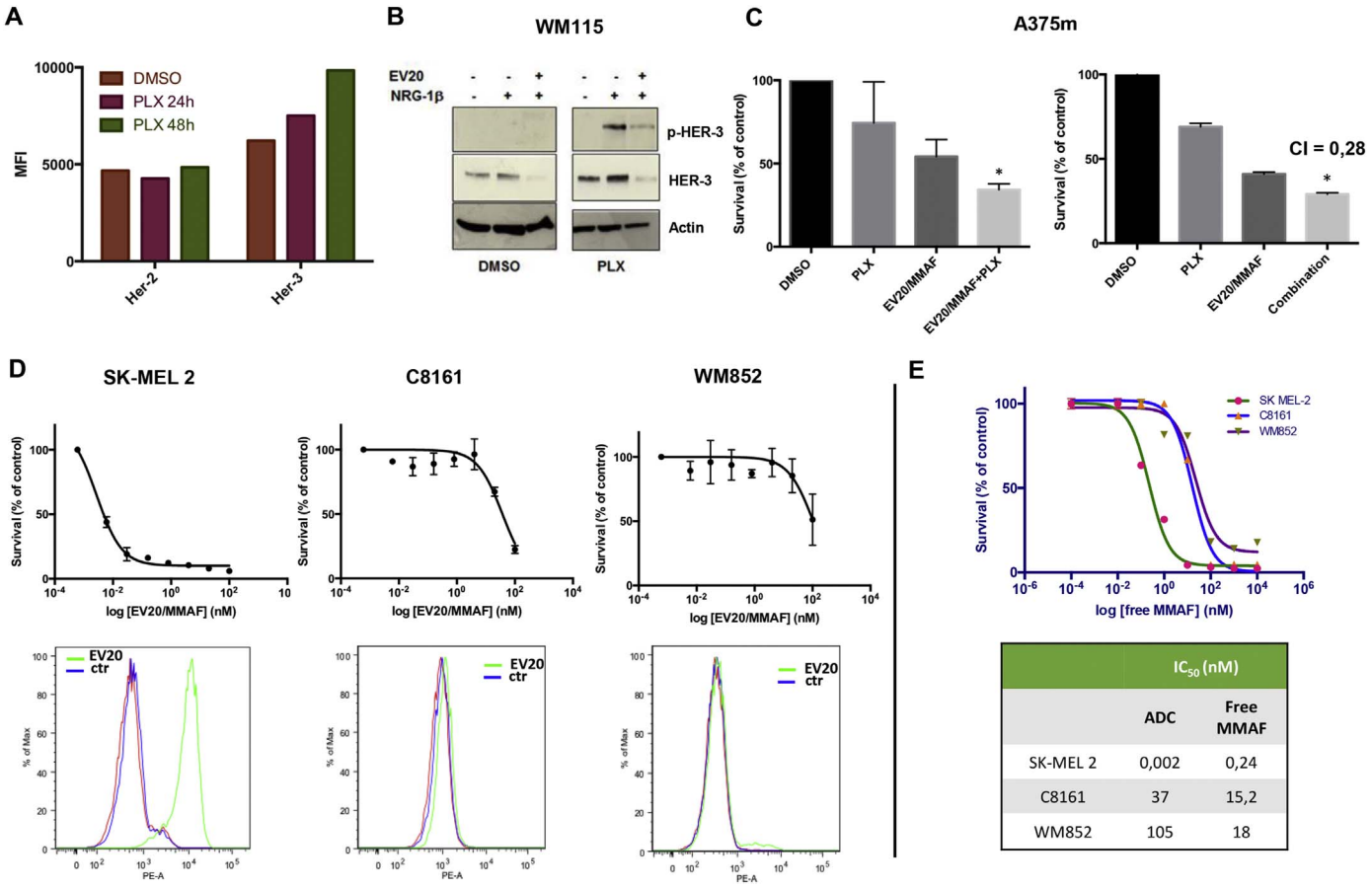

	IC_{50} (nM)	
	ADC	Free MMAF
SK-MEL 2	0,002	0,24
C8161	37	15,2
WM852	105	18

Fig. 3. EV20/MMAF activity is increased by prior exposure to PLX4720 and possesses cell killing activity independently of BRAF status.
(A) A375m cells were treated for 24 or 48 h with PLX4720 (1 μM) or DMSO as control. HER-3 and HER-2 surface expression were then evaluated by FACS analysis. (B) BRAF V600E WM115 cells were exposed overnight to DMSO or PLX4720 (1 μM). After wash out of the drug cells were pre-treated or not with EV20 (10 μg/ml) and then stimulated with NRG-1β (10 ng/ml) for 5 min. Cell lysates were blotted as indicated. (C) A375m cells were pre-treated overnight with DMSO or PLX4720 (1 μM). After wash out of the drug, cells were exposed to 0.16 nM EV20/MMAF for 120 h (left panel). A375m cells were co-exposed to 0.16 nM EV20/MMAF in combination with 0.1 μM of PLX4720 for 120 h and survival rate evaluated by MTT assay. Data are expressed as % survival over control. Mean +/− SD (n = 3). CI (combination index) value was calculated using Calcusyn software. (D) Cell killing activity of EV20/MMAF in BRAF wild type cells (SK-MEL 2, C8161, and WM852) was evaluated by MTT, after 120 h of treatment. Data are expressed as % survival over control. Mean +/− SD (n = 3). Lower panel shows HER-3 surface expression as evaluated by FACS. Cells were incubated with anti-HER-3 EV20 antibody followed by PE-goat anti-Human IgG staining. Red and blue curves represents unstained and no primary antibody stained (control) cells, respectively. (E) Cell killing activity of free MMAF in SK-MEL 2, C8161 and WM852 cells was evaluated by MTT assay, after 120 h of treatment. Data are expressed as % survival over control. Mean +/− SD (n = 3). Table indicates EV20/MMAF and free MMAF IC_{50} values calculated by GraphPad Prism 5 software. (For interpretation of the references to colour in this figure legend, the reader is referred to the web version of this article.)

Italian law (Authorization n° 292/2017-PR). Eight-weeks old male NSG mice (5–6 mice per group) were injected via the lateral tail vein with 5×10^5 A375m melanoma cells; the treatments (vehicle, vemurafenib, EV20/MMAF and combo) were started after 14 days from the injection. Vehicle (0,8% Tween80, 1% methylcellulose in H_2O) or vemurafenib (25 mg/kg) was given by oral gavage twice daily 5 days weekly for two weeks, EV20/MMAF (3.3 mg/kg) was administered intravenously once weekly for two weeks. After 30 days, mice were sacrificed, and lungs were processed for metastasis analysis. The animal health status was monitored daily and body weight was measured every 3–4 days during the treatment. At the end of experiment organs were harvested, fixed in 10% neutral buffered formalin, paraffin embedded, sectioned and stained with Hematoxylin and Eosin (BioOptica, Milan, Italy). To optimize the detection of microscopic metastases and ensure systematic uniform and random sampling, lungs and livers were cut transversally into 2.0 mm thick parallel slabs with a random position of the first cut in first 2 mm of the organ, resulting in 5–8 slabs for lungs and 6–8 slabs for livers. The slabs were then embedded cut surface down and sections were stained with Hematoxylin and Eosin. Slides were independently evaluated by two pathologists. To further assess in vivo ADC safety and potential adverse effects, NSG mice were treated with PBS or EV20/MMAF at the dose of 3.3 mg/kg and animal sacrificed after 15 days from drug injection. Major organs (heart, lungs, kidneys, liver and spleen) were harvested and analyzed by H&E staining.

3. Results

3.1. Generation and characterization of EV20/ADC

EV20 is an anti-HER-3 antibody which can be efficiently internalized by HER-3 expressing cancer cells, as previously reported [22,23]. With the aim to generate a novel ADC (EV20/MMAF) suitable for a potential clinical development, we have coupled EV20 to MMAF, a potent inducer of cell death by G2/M block which has been used to generate several ADCs currently tested in clinical trials [29]. EV20/MMAF was obtained via random conjugation through a non-cleavable linker. Conjugation report is attached in the Material section and a schematic representation of the ADC's generation is shown in Fig. 1A. Testing EV20/MMAF HER-3 binding and internalization rate gave near superimposable results to those obtained with naked EV20 (Fig. 1B–C). Interestingly, the murine anti-MMAF antibody was able to detect the intact MMAF-coupled but not the naked EV20 antibody (Fig. 1D). Next, we tested the cytotoxic activity of EV20/MMAF in vitro. To this end, A375m melanoma cells which express high levels of HER-3 and we

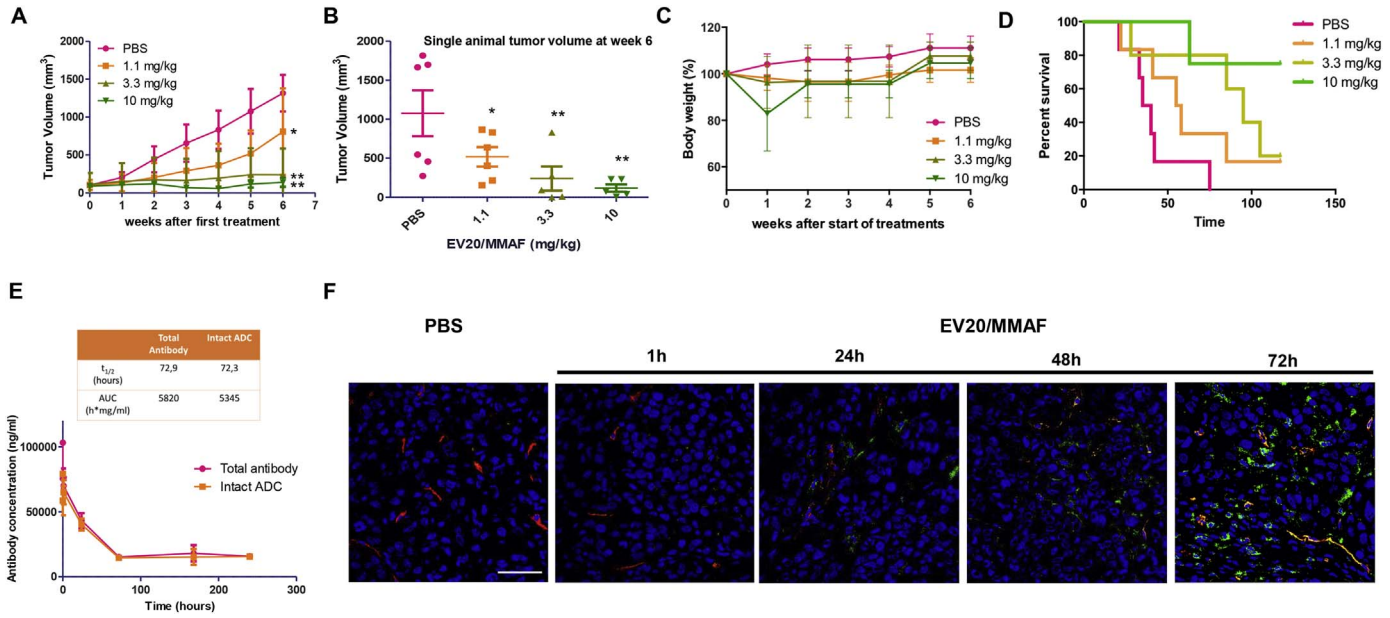

Fig. 4. EV20/MMAF treatment leads to a long lasting and dose dependent tumor growth inhibition and increased survival.
(A) Melanoma A375m xenografts were established by subcutaneous injection of 5×10^6 cells in immunodeficient CD1 mice. When tumors reached a volume of ~100 mm^3, mice were randomly grouped and therapeutic activity of EV20/MMAF evaluated by dose-response treatment. Control group (n = 6) received PBS, 1.1 mg/kg group (N = 6) and 3.3 mg/kg group (N = 5) received two injections of EV20/MMAF once/weekly, whilst the 10 mg/kg group (N = 6) received only one injection of EV20/MMAF. (B) Plot of single animals tumor volumes at week six. (C) Percent change of body weight in mice during the six weeks after the start of treatments. (D) Survival curve evaluated by Kaplan-Meier and analyzed by the log-rank test using Graphpad Prism 5 software. (E) Pharmacokinetic: non tumor-bearing CD1 nude mice were i.v. treated with a single dose of 3.3 mg/kg EV20/MMAF. Blood samples were collected and sandwich ELISAs were performed on sera to quantify total EV20 and intact EV20/MMAF concentrations. *p* values were determined by Student's *t*-test. $*p < 0.05$, $**p < 0.01$. (F) Representative images showing ADC accumulation in A375m tumor tissue after intravenously injection of EV20/MMAF (3.3 mg/kg) in relation to blood vessels, determined by immunofluorescence staining. After ADC was circulating for 1, 24, 48 or 72 h, tumor tissues were excised and subjected to immunofluorescence staining. EV20/MMAF was detected with anti-human IgG (green); blood vessels were stained using anti CD31/CD105 antibodies (red); cells nuclei were stained by DRAQ5 (blue). Scale bars: 50 μm. (For interpretation of the references to colour in this figure legend, the reader is referred to the web version of this article.)

showed to respond to EV20-Sap [24] were used. Cells were treated with EV20-Sap (72 h) or EV20/MMAF (48 h) and analyzed by Annexin staining or cell cycle analysis, respectively. As expected, a significant increase of Annexin staining was seen in cells exposed to EV20-Sap (being Saporin a well known inducer of apoptosis), while a massive G2/M block was observed in EV20/MMAF treated cells (Fig. 2A), confirming that EV20 antibody is a good vehicle for drug delivery. Next, to determine the cell killing potency of this novel compound, we performed a dose-response cytotoxic assay. A375m cells were incubated with increasing doses of EV20/MMAF for 120 h after which MTT staining was performed to analyze cell survival. The results of this experiment indicated that EV20/MMAF possesses a potent cell killing activity (IC_{50} = 0.014 nM) (Fig. 2B, left). Moreover, the observed cell killing activity was specific, as a 500-fold molar excess of naked EV20 resulted in the complete loss of activity (Fig. 2B, right). EV20/MMAF specificity was confirmed by the lack of response in mouse derived breast cancer TUBO cells (Fig. 2C) which express the murine form of HER-3 that is not recognized by the EV20 antibody, as previously reported [24]. Finally, ectopic expression of HER-3 sensitized to EV20/MMAF the otherwise resistant triple negative breast cancer cell line, MDA MB 231, expressing barely detectable HER-3 levels (Fig. 2D). All together, these observations show that EV20/MMAF is endowed with a potent and target-dependent cell killing activity.

3.2. EV20/MMAF cytotoxicity activity is independent to BRAF status

Our and other groups have recently demonstrated that HER-3 is upregulated in response to PLX4720 in BRAF mutated cells [10,30,31]. In line with this, we found that 48 h exposure of BRAF mutated A375m cells to PLX4720 resulted in approximately 40% increase of HER-3 expression, while no change was observed for HER-2 (Fig. 3A). Accordingly, in PLX4720 exposed cells, receptor ligand, NRG-1β, produced an increased HER-3 signaling, that was blocked by EV20 (Fig. 3B), thus confirming the ability of this antibody to inhibit receptor signaling, as previously reported [22,23,32].

From the above data, one would therefore expect that up regulation of HER-3 following BRAFi treatment results in an increased cell sensitivity to EV20/MMAF. Indeed, we found that the cytotoxic activity of EV20/MMAF, used at the suboptimal concentration of 0.16 nM was increased by overnight treatment of cells with PLX4720 (1 μM) (Fig. 3C, left panel). Moreover, prolonged treatment with a combination of EV20/MMAF (0.16 nM) and PLX4720 (0.1 μM) resulted in a synergistic effect, with a combination index of 0.28, suggesting the potential use of this ADC in BRAF mutated melanoma (Fig. 3C, right panel and Supplementary Fig. 1A).

To date, only 50% of melanomas bear BRAF mutations and are treated with vemurafenib. Therefore, we wondered whether EV20/MMAF activity is conserved in BRAF wild type melanoma. To this aim, EV20/MMAF cytotoxic activity was analyzed in three BRAF wild type cell lines expressing different levels of HER-3. SK-MEL 2 cells which express high levels of HER-3 resulted to be highly sensitive to EV20/MMAF (IC_{50} = 0.002 nM), whilst C8161 and WM852 cells, in which HER-3 expression is barely detectable, were insensitive to the agent (Fig. 3D). To further assess EV20/MMAF specificity, free MMAF cell killing activity was evaluated in HER-3 positive and HER-3 negative cells. Interestingly, cell killing activity of free MMAF in HER-3 positive SK-MEL 2 cells was lower compared to that of ADC (IC_{50} 0.24 nM vs 0.002 nM), demonstrating that EV20-mediated drug internalization increases the therapeutic activity of MMAF (being this in line with the low capacity of MMAF to permeate plasma membrane [33]). Conversely, free drug cytotoxicity in HER-3 negative (and not sensitive to EV20/MMAF) C8161 and WM852 cells resulted to be higher compared to that of ADC (IC_{50} 15.2 nM vs ≈ 37 nM for C8161; 18 nM vs ≈ 105 nM for WM852), further confirming that ADC, but not free

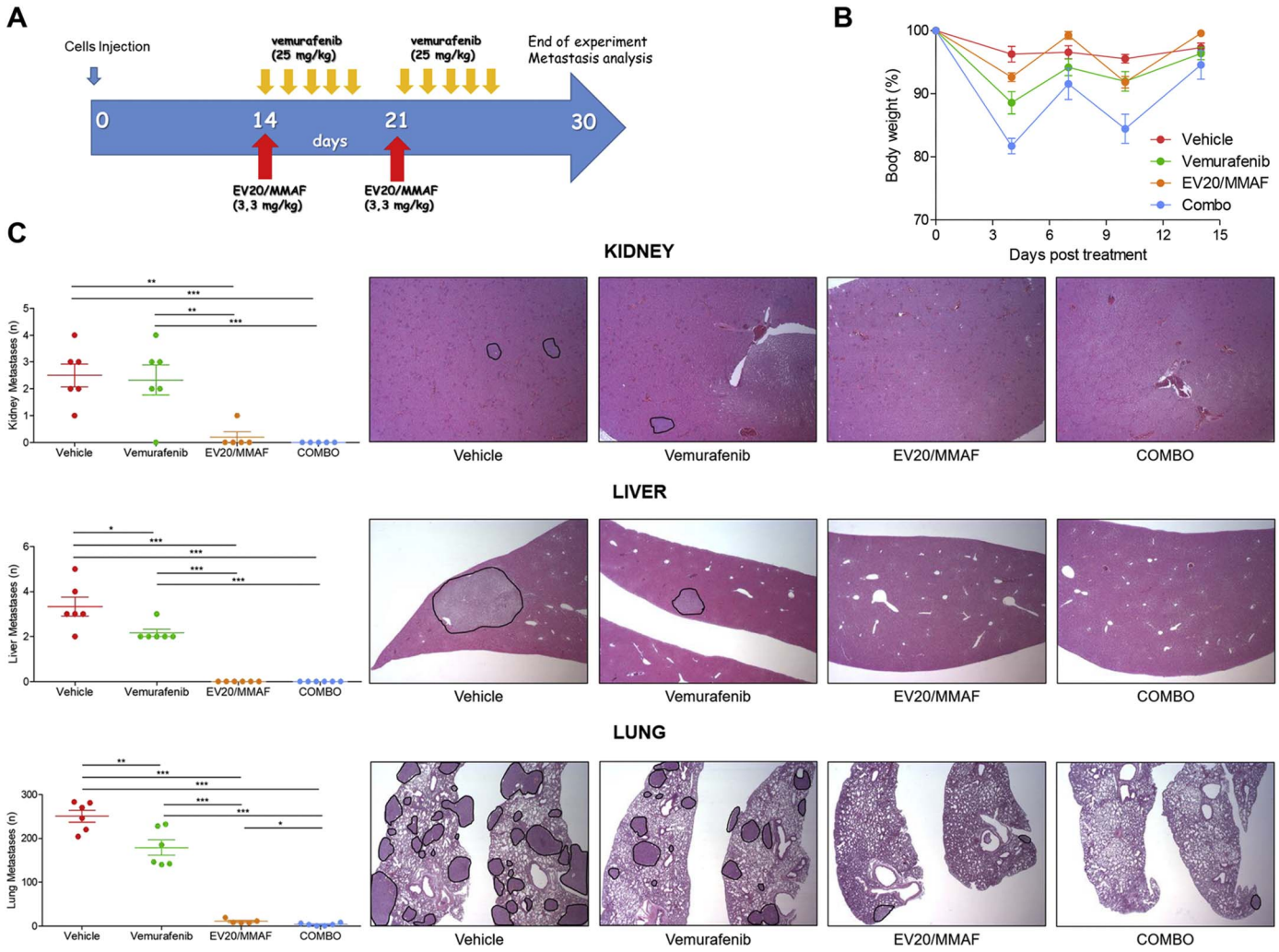

Fig. 5. EV20/MMAF shows superior activity of vemurafenib in vivo.
Experimental design is shown in (A). (B) Percent change of body weight of treated animals showing no significant treatment-related body weight loss. (C) Kidney, liver and lungs harvested from mice of control and treated groups, were stained with Hematoxylin and Eosin protocol for metastatic loci analysis. All melanoma metastatic lesions were analyzed and plotted on graphs (left). Representative images are shown (right).

MMAF cell killing activity, is dependent on HER-3 expression (Fig. 3E).

All together, these results suggest that HER-3 expressing melanoma cells can be targeted by EV20/MMAF, independently of BRAF status.

3.3. EV20/MMAF therapeutic activity

Having demonstrated that EV20/MMAF possesses a potent and specific antitumor activity in vitro, we analyzed the therapeutic efficacy of this ADC in vivo using the A375m melanoma xenograft model. Once tumors reached a volume of approximately 100 mm^3, mice were divided in four groups (n = 6) and treated with increasing doses of EV20/MMAF (1.1–3.3 and 10 mg/kg) for a total of two administrations. Animals injected with PBS served as a control group. This dose-response study showed that EV20/MMAF possesses a potent and dose-dependent antitumor activity (Fig. 4A–B) with no associated toxicity, as evidenced by evaluating mice's body weight (Fig. 4C), with the exception of the higher dose (10 mg/kg) which was injected only once, since mice exhibited nearly 20% loss of body weight, following the first dose. Of note, this single injection was sufficient to promote a long-lasting antitumor response associated with a significant increased survival and no further toxicity effects were observed after the suspension of treatment (Fig. 4C-D). The kinetic profiles of total EV20 and intact EV20/MMAF, evaluated in nude mice not harboring tumors were quite similar in terms of $t_{1/2}$ and AUC values (Fig. 4E). Interestingly, LC-MS analysis revealed that free MMAF is not released in mice serum (data not shown). Moreover, we observed a time-dependent accumulation of EV20/MMAF in tumor tissues indicating ADC accessibility to the target cells in vivo (Fig. 4F).

Our previous published and unpublished data revealed that the highly metastatic A375m melanoma cells, once introduced in the blood stream, take about 25–35 days to form metastatic lesions in the main organs, such as lungs, liver and kidneys, therefore providing an excellent model to study the effect of a drug on metastatic spreading. We therefore asked whether combination of EV20/MMAF and vemurafenib could result in a more effective anti-metastatic activity in vivo. To this aim, an experimental metastasis assay based on injection of BRAFV600E A375m cells in the tail vein of immunocompromised NSG mice was used. After cells injection, mice were divided in four arms and treated with the anti-tumor agents either singly or in combination as indicated in schematic representation of Fig. 5. ADC was used at the dose of 3.3 mg/kg which resulted from the previous xenograft experiment to be highly active and well tolerated, while for vemurafenib a suboptimal dose of 25 mg/kg was used, as previously reported [34]. At the end of the experiment, mice were sacrificed and the number of metastatic foci analyzed by IHC.

All vehicle-treated animals displayed a high number of metastatic lesions that were reduced by vemurafenib treatment. Surprisingly, two injections of EV20/MMAF were sufficient to inhibit almost completely

metastasis formation in all analyzed organs. Therefore, no further increase in therapeutic efficacy could be obtained in animals receiving the combination treatment, indicating that EV20/MMAF possesses a higher therapeutic efficacy compared to vemurafenib. Of note, no organ toxicity was observed in major organs (lungs, heart, liver, kidneys and spleen) of treated animals after 15 days (Supplementary Fig. 1C).

4. Discussion

CM is a lethal form of skin cancer whose incidence rates are steadily growing in western countries (National Cancer Institute. Surveillance, Epidemiology and End Results. http://www.seer.cancer.gov/statfacts/ (accessed November 30, 2017). Although early stage CM can be efficiently cured by surgery, advanced melanoma represents a serious public health problem. Indeed, for patients which are diagnosed with regional or distant metastasis, 5-year overall survival rate is below 20% [35,36]. Increased incidence combined with a decrease of survival rate in advanced CM pushes towards the development of novel therapeutics. In this respect, a sensible improvement in the treatment of the disease has been achieved with the introduction of immune and targeted therapies in combination with chemotherapy, which was, up to twenty years ago, the only standard of care for the metastatic disease. Targeted therapies for advanced CM consist of BRAF and MAPK inhibitors which have been developed to target BRAF mutated CM which represent almost 50% of all melanoma cases. While a response rate of up to 70% has been observed with first-line BRAF/MEK inhibitors, the duration of response is limited, as disease progression is observed within 1 year from the start of treatment. This limited duration of response to BRAF/MEK inhibitors is mainly due to acquired resistance to the drugs. HER-3 up-regulation has been shown to represent a drive escape mechanism in breast cancer cells treated with trastuzumab or PI3K inhibitors as well as in melanoma or colorectal carcinoma cells exposed to BRAF or MEK inhibitors, or gastric cancer cells treated with MET inhibitors [7–12].

We have recently shown that HER-3, though at different levels, is expressed homogeneously in a high percentage (76%) of metastatic melanoma lesions and demonstrated that melanoma cells expressing HER-3 can be targeted by an ADC based on the internalizing anti-HER-3 antibody EV20 carrying the plant toxin *Saporin* [24]. While this represented a proof of principle and a good starting point, the potential use of this approach in the clinic requires the development of a different payload. To this end, we generated a novel EV20-based ADC by coupling the antibody to the tubulin polymerization inhibitor monomethyl auristatin F (MMAF), a cytotoxic drug used to generate multiple ADCs currently tested in clinical trials. In the present study, we demonstrate that EV20/MMAF is capable of specifically and efficiently targeting melanoma cells. Importantly, we found that cell killing activity of this novel ADC is independent of BRAF status of the cells. The antitumor response was complete and durable both in the xenograft and the metastasis model. Importantly, EV20/MMAF was highly stable and free drug was not detected in mice's circulation. Moreover, the novel ADC was well tolerated and no signs of systemic toxicity were seen in treated animals.

The payload used in the present study, MMAF, is known to possess a low bystander activity [33] and presumably the ADC is not endowed with the ability to target HER-3 negative cells. However, in tumor xenografts used in the present study originated by an immortalized cell line, homogenous expression of HER-3 within the tumor mass is expected. By contrast, tumors derived by patients are known to be heterogeneous, and HER-3 expression might occur only in a fraction of tumor cells. Therefore, it is possible to speculate that the therapeutic activity of an EV20-based ADC can be increased using payloads endowed with a bystander activity (e.g. MMAE), which might be able to target HER-3 negative cells as well. In this respect, our data showing that free MMAF is not released in the circulation may represent a basis for the generation of an EV20-based ADC using the same linker but a payload with a higher bystander activity.

In sum, this study proposes EV20/MMAF as a new ADC with promising therapeutic efficacy, warranting extensive pre-clinical evaluation in melanoma with high levels of HER-3 expression.

Supplementary data to this article can be found online at https://doi.org/10.1016/j.jconrel.2018.03.016.

Conflict of interests

GS and SI are shareholders of Mediapharma s.r.l.; The other authors have no potential conflict of interest to disclose.

Acknowledgments

We are indebted to Prof. Alex Ullrich (Max-Planck Institute, Martinsried, Germany) for providing melanoma cells used in this study. We thank Rossana La Sorda and Annalisa Nespoli for technical assistance.

Funding

This project was fundend in part by Mediapharma Srl; SI is supported by a grant from Ministero della Sanità, Ricerca Finalizzata 2011/2012 (PE-2011-02347028); VDL is supported by AIRC (IG:20043); EC is recipient of an AIRC fellowship; GS is supported by AIRC (IG:18467).

References

[1] E.A. Rozeman, T.J.A. Dekker, J. Haanen, C.U. Blank, Advanced melanoma: current treatment options, biomarkers, and future perspectives, Am. J. Clin. Dermatol. (2017).
[2] A.M. Eggermont, A. Spatz, C. Robert, Cutaneous melanoma, Lancet 383 (2014) 816–827.
[3] A.K. Karlsson, S.N. Saleh, Checkpoint inhibitors for malignant melanoma: a systematic review and meta-analysis, Clin. Cosmet. Investig. Dermatol. 10 (2017) 325–339.
[4] R. Kudchadkar, K.H. Paraiso, K.S. Smalley, Targeting mutant BRAF in melanoma: current status and future development of combination therapy strategies, Cancer J. 18 (2012) 124–131.
[5] Z. Karoulia, E. Gavathiotis, P.I. Poulikakos, New perspectives for targeting RAF kinase in human cancer, Nat. Rev. Cancer 17 (2017) 676–691.
[6] R. Roskoski, The ErbB/HER family of protein-tyrosine kinases and cancer, Pharmacol. Res. 79 (2014) 34–74.
[7] N. Gaborit, M. Lindzen, Y. Yarden, Emerging anti-cancer antibodies and combination therapies targeting HER3/ERBB3, Hum. Vaccin. Immunother. (2015) 1–17.
[8] E. Capone, P.R. Prasetyanti, G. Sala, HER-3: hub for escape mechanisms, Aging (Albany NY) 7 (2015) 899–900.
[9] J. Ma, H. Lyu, J. Huang, B. Liu, Targeting of erbB3 receptor to overcome resistance in cancer treatment, Mol. Cancer 13 (2014) 105.
[10] E.V. Abel, K.J. Basile, C.H. Kugel, A.K. Witkiewicz, K. Le, R.K. Amaravadi, G.C. Karakousis, X. Xu, W. Xu, L.M. Schuchter, J.B. Lee, A. Ertel, P. Fortina, A.E. Aplin, Melanoma adapts to RAF/MEK inhibitors through FOXD3-mediated upregulation of ERBB3, J. Clin. Invest. 123 (2013) 2155–2168.
[11] Enhanced ERBB3 Signaling Promotes Resistance in Melanoma, Cancer Discov. 3 (2013) 479.
[12] A. Chakrabarty, V. Sanchez, M.G. Kuba, C. Rinehart, C.L. Arteaga, Feedback upregulation of HER3 (ErbB3) expression and activity attenuates antitumor effect of PI3K inhibitors, Proc. Natl. Acad. Sci. U. S. A. 109 (2012) 2718–2723.
[13] K. Gala, S. Chandarlapaty, Molecular pathways: HER3 targeted therapy, Clin. Cancer Res. 20 (2014) 1410–1416.
[14] L. Aurisicchio, E. Marra, L. Luberto, F. Carlomosti, C. De Vitis, A. Noto, Z. Gunes, G. Roscilli, G. Mesiti, R. Mancini, M. Alimandi, G. Ciliberto, Novel anti-ErbB3 monoclonal antibodies show therapeutic efficacy in xenografted and spontaneous mouse tumors, J. Cell. Physiol. 227 (2012) 3381–3388.
[15] N. Gaborit, M. Lindzen, Y. Yarden, Emerging anti-cancer antibodies and combination therapies targeting HER3/ERBB3, Hum. Vaccin. Immunother. 12 (2016) 576–592.
[16] A. Beck, L. Goetsch, C. Dumontet, N. Corvaia, Strategies and challenges for the next generation of antibody-drug conjugates, Nat. Rev. Drug Discov. 16 (2017) 315–337.
[17] C. Martin, C. Kizlik-Masson, A. Pelegrin, H. Watier, M.C. Viaud-Massuard, N. Joubert, Antibody-drug conjugates: design and development for therapy and imaging in and beyond cancer, LabEx MAbImprove industrial workshop, July 27-28, 2017, Tours, France, MAbs 0 (2017).
[18] A. Nagayama, L.W. Ellisen, B. Chabner, A. Bardia, Antibody-drug conjugates for the treatment of solid tumors: clinical experience and latest developments, Target. Oncol. 12 (2017) 719–739.
[19] A. Thomas, B.A. Teicher, R. Hassan, Antibody-drug conjugates for cancer therapy, Lancet Oncol. 17 (2016) e254–262.

[20] K.L. Moek, D.J.A. de Groot, E.G.E. de Vries, R.S.N. Fehrmann, The antibody-drug conjugate target landscape across a broad range of tumour types, Ann. Oncol. 28 (2017) 3083–3091.
[21] C. Peters, S. Brown, Antibody-drug conjugates as novel anti-cancer chemotherapeutics, Biosci. Rep. 35 (2015).
[22] G. Sala, S. Traini, M. D'Egidio, G. Vianale, C. Rossi, E. Piccolo, R. Lattanzio, M. Piantelli, N. Tinari, P.G. Natali, R. Muraro, S. Iacobelli, An ErbB-3 antibody, MP-RM-1, inhibits tumor growth by blocking ligand-dependent and independent activation of ErbB-3/Akt signaling, Oncogene 31 (2012) 1275–1286.
[23] G. Sala, I.G. Rapposelli, R. Ghasemi, E. Piccolo, S. Traini, E. Capone, C. Rossi, A. Pelliccia, A. Di Risio, M. D'Egidio, N. Tinari, R. Muraro, S. Iacobelli, C.I.N.P.L.B.-O. (CINBO), EV20, a novel anti-ErbB-3 humanized antibody, promotes ErbB-3 down-regulation and inhibits tumor growth in vivo, Transl. Oncol. 6 (2013) 676–684.
[24] E. Capone, F. Giansanti, S. Ponziani, A. Lamolinara, M. Iezzi, A. Cimini, F. Angelucci, R. Sorda, V. Laurenzi, P.G. Natali, R. Ippoliti, S. Iacobelli, G. Sala, EV20-sap, a novel anti-HER-3 antibody-drug conjugate, displays promising anti-tumor activity in melanoma, Oncotarget 8 (2017) 95412–95424.
[25] S. Rovero, A. Amici, E. Di Carlo, R. Bei, P. Nanni, E. Quaglino, P. Porcedda, K. Boggio, A. Smorlesi, P.L. Lollini, L. Landuzzi, M.P. Colombo, M. Giovarelli, P. Musiani, G. Forni, DNA vaccination against rat her-2/Neu p185 more effectively inhibits carcinogenesis than transplantable carcinomas in transgenic BALB/c mice, J. Immunol. 165 (2000) 5133–5142.
[26] S. Anastasi, L. Fiorentino, M. Fiorini, R. Fraioli, G. Sala, L. Castellani, S. Alema, M. Alimandi, O. Segatto, Feedback inhibition by RALT controls signal output by the ErbB network, Oncogene 22 (2003) 4221–4234.
[27] T.C. Chou, P. Talalay, Quantitative analysis of dose-effect relationships: the combined effects of multiple drugs or enzyme inhibitors, Adv. Enzym. Regul. 22 (1984) 27–55.
[28] T.C. Chou, Theoretical basis, experimental design, and computerized simulation of synergism and antagonism in drug combination studies, Pharmacol. Rev. 58 (2006) 621–681.
[29] B.E. de Goeij, J.M. Lambert, New developments for antibody-drug conjugate-based therapeutic approaches, Curr. Opin. Immunol. 40 (2016) 14–23.
[30] P.R. Prasetyanti, E. Capone, D. Barcaroli, D. D'Agostino, S. Volpe, A. Benfante, S. van Hooff, V. Iacobelli, C. Rossi, S. Iacobelli, J.P. Medema, V. De Laurenzi, G. Sala, ErbB-3 activation by NRG-1beta sustains growth and promotes vemurafenib resistance in BRAF-V600E colon cancer stem cells (CSCs), Oncotarget 6 (2015) 16902–16911.
[31] C. Montero-Conde, S. Ruiz-Llorente, J.M. Dominguez, J.A. Knauf, A. Viale, E.J. Sherman, M. Ryder, R.A. Ghossein, N. Rosen, J.A. Fagin, Relief of feedback inhibition of HER3 transcription by RAF and MEK inhibitors attenuates their antitumor effects in BRAF-mutant thyroid carcinomas, Cancer Discov. 3 (2013) 520–533.
[32] R. Ghasemi, I.G. Rapposelli, E. Capone, C. Rossi, R. Lattanzio, M. Piantelli, G. Sala, S. Iacobelli, Dual targeting of ErbB-2/ErbB-3 results in enhanced antitumor activity in preclinical models of pancreatic cancer, Oncogene 3 (2014) e117.
[33] S.O. Doronina, B.A. Mendelsohn, T.D. Bovee, C.G. Cerveny, S.C. Alley, D.L. Meyer, E. Oflazoglu, B.E. Toki, R.J. Sanderson, R.F. Zabinski, A.F. Wahl, P.D. Senter, Enhanced activity of monomethylauristatin F through monoclonal antibody delivery: effects of linker technology on efficacy and toxicity, Bioconjug. Chem. 17 (2006) 114–124.
[34] H. Yang, B. Higgins, K. Kolinsky, K. Packman, W.D. Bradley, R.J. Lee, K. Schostack, M.E. Simcox, S. Kopetz, D. Heimbrook, B. Lestini, G. Bollag, F. Su, Antitumor activity of BRAF inhibitor vemurafenib in preclinical models of BRAF-mutant colorectal cancer, Cancer Res. 72 (2012) 779–789.
[35] C.M. Balch, J.E. Gershenwald, S.J. Soong, J.F. Thompson, M.B. Atkins, D.R. Byrd, A.C. Buzaid, A.J. Cochran, D.G. Coit, S. Ding, A.M. Eggermont, K.T. Flaherty, P.A. Gimotty, J.M. Kirkwood, K.M. McMasters, M.C. Mihm Jr., D.L. Morton, M.I. Ross, A.J. Sober, V.K. Sondak, Final version of 2009 AJCC melanoma staging and classification, J. Clin. Oncol. 27 (2009) 6199–6206.
[36] E.L. Korn, P.Y. Liu, S.J. Lee, J.A. Chapman, D. Niedzwiecki, V.J. Suman, J. Moon, V.K. Sondak, M.B. Atkins, E.A. Eisenhauer, W. Parulekar, S.N. Markovic, S. Saxman, J.M. Kirkwood, Meta-analysis of phase II cooperative group trials in metastatic stage IV melanoma to determine progression-free and overall survival benchmarks for future phase II trials, J. Clin. Oncol. 26 (2008) 527–534.